Available online at www.sciencedirect.com
ScienceDirect
J. Biochem. Biophys. Methods 70 (2007) 627–633
JOURNAL OF biochemical and biophysical methods
www.elsevier.com/locate/jbbm

A combined micro-resonance Raman and absorption set-up enabling *in vivo* studies under varying physiological conditions: The nerve globin in the nerve cord of *Aphrodite aculeata*

K. Ramser [a,d,*], W. Wenseleers [b,*], S. Dewilde [c], S. Van Doorslaer [b], L. Moens [c], D. Hanstorp [a]

[a] *Department of Physics, Göteborgs University, SE-412 96 Göteborg, Sweden*
[b] *Department of Physics, University of Antwerp, Universiteitsplein 1, B2610 Antwerpen, Belgium*
[c] *Department of Biomedical Sciences, University of Antwerp, Universiteitsplein 1, B2610 Antwerpen, Belgium*
[d] *Department of Computer Science and Electrical Engineering, Luleå University of Technology, SE-971 87 Luleå, Sweden*

Received 13 June 2006; received in revised form 22 January 2007; accepted 21 February 2007

Abstract

We hereby report on the design of a set-up combining micro-resonance Raman and absorption spectroscopy with a microfluidic system. The set-up enabled us to study the nerve globin of *Aphrodite aculeata* in the functional isolated nerve cord under varying physiological conditions for extended periods of time. The oxygenation cycle of the organism was triggered by utilizing the microfluidic system that allowed for a fast switch between aerobic and anaerobic conditions. The nerve globin was found to very easily shift from a penta-coordinated high spin ferrous form to the oxy state upon a change from anaerobic to aerobic conditions. The observed fast reaction to varying O_2 concentrations supports an oxygen-carrying and/or -storing function of the nerve globin. In addition, by combining resonance Raman and absorption spectroscopy, the physiological response could be distinguished from light-induced effects.

Keywords: Micro-resonance Raman spectroscopy; Absorption spectroscopy; Microfluidic system; Nerve globin; *Aphrodite aculeata*

1. Introduction

Hemoglobins (Hbs) are found in many living organisms including bacteria, plants, vertebrates and invertebrates. They have been studied in detail over centuries, but still, new functions and new varieties of Hbs are discovered [1,2]. An extensive review by Weber and Vinogradov elucidates the versatility of non-vertebrate Hbs, their functions and molecular adaptations [3]. Structurally, these proteins occur in many types, ranging from monomeric to multi-domain subunits with a weight from 17 to 1700 kDa. The overall amino acid sequences vary widely, almost randomly, but apart from the globin fold certain features are always conserved, such as the invariant residues Phe at position CD1 and His at F8, and the characteristic patterns of hydrophobic domains in each of the α-helical residues. The physiological functions of invertebrate Hbs are much more diverse than in vertebrates. Storage and transport of O_2 is the most obvious one, but apart from that, known functions include facilitation of O_2 diffusion, O_2 scavenging, O_2 sensing, oxidase activity, peroxidase activity for detoxification, and NO regulation and metabolism, only to name a few [3].

The expression of several Hbs in tissue and in the ganglia of the nerve cords in several invertebrates is nowadays well established. Still, they are far from common and can be present or absent in closely related species. This study concentrates on a nerve globin found in the tissue of the chain of nerve ganglia of the polychaete annelid *Aphrodite aculeata*. The heme in the nerve cord was discovered as early as 1872 by Lankester. He describes a “bright crimson tint colour as intense as in a drop of fresh blood” [4]. A hundred years later, studies showed that the

* Corresponding authors. Wenseleers is to be contacted at Department of Physics, University of Antwerp, Wilrijk-Antwerp, Belgium. Tel.: +32 3 820 24 51; fax: +32 3 820 24 70. Ramser, Department of Computer Science and Electrical Engineering, Luleå University of Technology, SE-971 87 Luleå, Sweden. Tel.: +46 920 49 16 48; fax: +46 920 49 31 11.
E-mail addresses: kerstin.ramser@ltu.se (K. Ramser), Wim.Wenseleers@ua.ac.be (W. Wenseleers).

0165-022X/$ - see front matter © 2007 Elsevier B.V. All rights reserved.
doi:10.1016/j.jbbm.2007.02.003

nerve globin has a molecular weight (MW) of approximately 17 kDa with a hyperbolic oxygen dissociation curve (P50=1.1 mm Hg) [5,6]. In 1996, the kinetics of ligand-binding of the purified nerve globin and its primary structure were carefully investigated [7]. The primary structure confirmed that the globin is intracellular, of a tissue or myoglobin (Mb) type, and that it matches both vertebrate and non-vertebrate templates quite well. The investigations of the ligand-binding kinetics showed that the oxygen association rates are among the highest observed, approaching the diffusion limit. The dissociation rate is also relatively high, resulting in an average oxygen affinity, as found in Hb or Mb. The abundance, the intracellular location and the functional characteristics of the homomeric, penta-coordinated nerve globin point towards an oxygen storage and transport function. Recently, a detailed analysis of the oxygenation characteristics on the purified protein was published [8].

The so far found features of the nerve globin awaken the interest to study the action potential of the nerve cord in relation to the oxygenation of the nerve globin under aerobic and anaerobic environments. Since the annelid lives under oxygen poor conditions, the nerve globin might have an essential role on the functioning of the nerve cord. A comparable observation has been reported previously for similar systems by Kraus and Colacino [9]. They found that depending on the presence of a nerve globin in the nerve cord the activity of the action potential could be increased by approximately one order of magnitude.

Motivated by this idea, we were interested in finding optimum conditions to study the reactions of the nerve globin to environmental changes under *in vivo* conditions with micro-resonance Raman and absorption techniques. Both methods have been used extensively to study heme proteins *in vitro* as well as *in vivo* and give an excellent opportunity to study the reactivity of the nerve globin to environmental stimuli in its natural milieu and to learn more about its function. Therefore, we designed and built a microscope connected to both a resonance Raman and a UV–Vis spectrometer that was equipped with a microfluidic system allowing a fast change of the physiological conditions of the nerve cord.

The current study is meant as a proof-of-principle test to demonstrate that the study of globins in an isolated nerve cord is feasible. Spectral changes induced by alterations in the gas environment could be monitored in real time. This opens up the path for many interesting future applications, as described above. Furthermore, up to now investigations on this particular nerve globin have been carried out mainly on purified proteins. Consequently, *in vivo* experiments might lead to new findings about its functions and physiological role. The advantages and disadvantages of this approach will be discussed.

2. Materials and methods

2.1. The microfluidic system

Microfluidic systems have become vital tools for biological and chemical analysis. They give control over the diffusion of substances and chemical reactions, mimicking *in vivo* conditions in an *in vitro* environment [10–12]. The micro laboratories give the possibility to control and manipulate small sample volumes and monitoring chemical reactions in real time. Such a lab-on-a-chip can easily be integrated into existing experimental set-ups due to the minimal size. Hence, in order to control the environment of the sample used in this study, a tightly sealed flow cell was used that could be put onto a microscope slide. A continuous pump was connected to a switch leading to two different seawater-containing vessels purged with air, He or N_2. The seawater was flushed through the flow cell by the pump. The flow cell consisted of a sealed Plexiglas cell (ø=5 mm, h=0.5 mm) with an in- and outlet. By doing so, anaerobic or aerobic conditions could be created in the flow cell and resultant changes in spectra could be monitored. The flow through the cell was 5 µl/min and the volume was 0.01 cm^3 ($\pi \cdot 0.25^2 \cdot 0.05$ cm^3). The buffer also has to pass the tubing through the pump-system, which has a length of 1 m and a diameter of 0.5 mm, thus the exchange of seawater in the cell takes approximately 3 min.

2.2. Design of the experimental set-up

The aim of the experimental set-up was to combine the microfluidic system and the microscope with a macro-resonance Raman and an absorption spectrometer. A scheme of the set-up is shown in Fig. 1. The absorption spectra were obtained through white light illumination and recorded by a UV–Vis-NIR grating spectrometer with a CCD detector (Ocean Optics, HR2000 with 300 lines/mm grating), connected to the microscope. To enable sequential monitoring of the absorption spectra, a glass-plate on a movable flip-flop mount was used to reflect the white light to the grating spectrometer. The light was first guided through a pinhole (iris) to decrease the collection area of the sample to a diameter of approximately 20 µm in order to block possible background signal and then through a lens to focus the light into the spectrometer.

A Kr-ion laser tuned to 413.1 nm was used to excite the sample. The laser light was reflected nearly 100% into the microscope by a dichroic mirror (DM1) that transmits the rest of the visible spectrum from 450 nm to the near infrared. The excitation and back-scattering collection system consisted of a home-built inverted microscope, equipped with a 60× water-immersion objective (NA=1.2) coupled to the Dilor XY-800 Raman spectrometer. The Raman back-scattered light was reflected into the spectrometer by a second dichroic mirror (DM2). This dichroic mirror transmitted the 413 nm line to ~40% while it reflected >90% between 420 and 520 nm. The spectra were recorded by a liquid-nitrogen-cooled CCD. The sample was also imaged by a CCD-chip from a digital camera coupled to a PC.

2.3. Resonance Raman and UV–Vis spectroscopy of heme proteins

The vibrational modes of the chromophoric heme group are selectively enhanced when applying resonance Raman spectroscopy on heme proteins, and information of conformational changes and/or changes in the spin and oxidation state of the

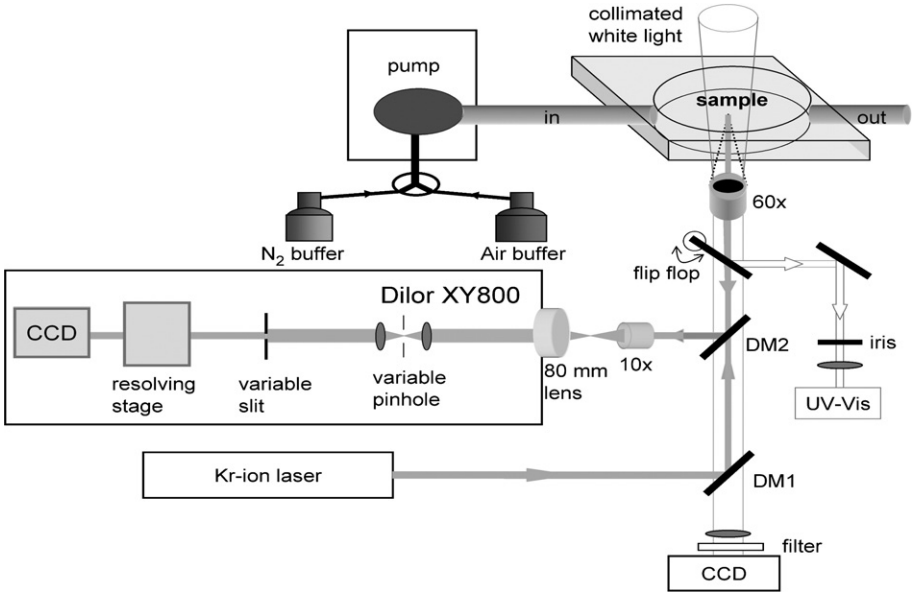

Fig. 1. Scheme of the set-up: The Raman excitation line from a Kr^{+}-ion laser (413.1 nm) is reflected by a dichroic mirror (DM1) into an inverted microscope objective (60× water-immersion). The back-scattered Raman signal is re-collected by the same objective and reflected into the Raman spectrometer by a dichroic mirror (DM2), passing a 10× objective in order to optimize the overfilling of the grating in the resolving stage. Absorption spectra are excited through a halogen lamp (emission 430–650 nm). The signal is reflected to the UV–Vis spectrometer by a glass-plate mounted on a flip-flop mirror, passing a pinhole and a lens to increase the S/N-ratio. The sample, monitored by a CCD-chip from a digital camera, is mounted in a tightly sealed flow cell connected to a HPLC pump with a switch connected to seawater vessels purged with air, He or N_2.

iron can be gained. Moreover, if the resonance effect is high enough, it is possible to look at a molecule of interest without interference by surrounding media or other components of the sample [13–15]. The concentration of the nerve globin found in the glial cells of the ganglia and the ventral nerve cord in *A. aculeata* is in the millimolar range [16], which is sufficient to perform resonance Raman on the intact and isolated nerve cord. It is well established that the ν_4, ν_3 and ν_2 bands in the high-frequency region (between 1350–1700 cm^{-1}) of the resonance Raman spectrum are sensitive to the oxidation state, spin state and coordination number of the heme iron. Here, the ν_3 and the ν_4 will be discussed. The ν_3 mode (1470–1520 cm^{-1}) is sensitive to both the axial coordination and spin state of the iron. The ν_4 band in the 1350–1400 cm^{-1} region is susceptible to the π-electron density of the heme and thus to the oxidation state of the iron [17]. Specifically, when the heme is in a five-coordinated ferrous high spin state, the ν_4 band is found at 1356 cm^{-1} and the ν_3 band at 1470 cm^{-1}. In the ferrous six-coordinated low spin form the ν_4 band is found at 1361 cm^{-1} and ν_3 at 1493 cm^{-1}, while for the six-coordinated ferric low spin form, the ν_4 band shifts to 1374 cm^{-1}, and the ν_3 to 1505 cm^{-1}. Note, that the ν_3 and the ν_4 values are almost identical for the His-Fe^{2+}–O_2 and the His-Fe^{2+}CO form [14,15,18].

The absorption spectra of heme proteins are characterized by different bands due to transitions between the electronic states of the π* electrons in the porphyrin ring, namely the Soret band in the 390 to 450 nm wavelength region and the Q bands in the visible region between 500 and 650 nm [7]. The latter are very sensitive to changes in oxidation and ligation of the heme iron. The absorption spectra of the different states of the nerve globin have been published before [7]. The deoxy form displays a shoulder at 550 nm, next to the maximum at 569 nm. The oxy form displays two maxima at 545 nm and 575 nm. The met form has two broad maxima at 505 nm and at 640 nm [7].

Each Raman and UV–Vis experiment was repeated simultaneously at least 5 times to guarantee reproducibility.

2.4. Fluorometer

The fluorescence spectrum was measured in the emission scan mode with a Varian Cary Eclipse fluorometer in the wavelength region between 455 to 800 nm. The excitation and emission slit were set to 5 nm with a data interval of 1 nm and an averaging time of 0.5 s. The excitation and emission filters of the spectrometer were replaced by suitable interference and glass filters.

2.5. Sample preparation

The nerve cord was dissected and isolated from the polychaete annelid *A. aculeata*, and was put directly into the flow cell filled with fresh seawater. Care was taken that the nerve cord did not dry out. Measurements were started immediately after the sample had been mounted.

3. Results

3.1. The resonance Raman spectrum of the nerve globin of A. aculeata

To our knowledge, there is so far no literature on the resonance Raman spectra measured in the nerve cord under *in vivo* conditions of the nerve globin found in the polychaete

A. aculeata. The first step in our analysis therefore consisted of recording the resonance Raman spectra of both the deoxy and the oxy form of the functioning nerve globin. In order to get the protein to change from the oxygenated to the deoxygenated form, the nerve cord was exposed to aerobic or anaerobic buffer. The spectra taken from a ganglion of the dissected and isolated nerve cord are shown in Fig. 2. The ν_3 and ν_4 lines for the deoxy form at 1474 and 1361 cm^{-1}, respectively, indicate the presence of a five-coordinate low spin heme [19]. This is similar to what is observed for invertebrate Hb and Mb [20], but contrasts the findings for Neuroglobin, which is a recently discovered vertebrate nerve globin [21,22]. The latter globin exhibits six-coordination in both the ferrous and ferric state, whereby the distal E7 histidine ligand occupies the sixth coordination site. The *in vitro* auto oxidation rate of the nerve globin under study was found to be in the typical range of Hb and Mb, indicating no stability problems [23]. The absence of the met form in the *in vivo* absorption spectra confirms this stability.

3.2. Investigation of the nerve globin under varying aerobic conditions

In order to study the *in vivo* influence of a changing oxygen concentration on the nerve globin in the nerve cord, the nerve cord was put in a sealed flow cell flushed with seawater purged either with air or He. Different time series of absorption and resonance Raman spectra were taken as a function of the flushing conditions.

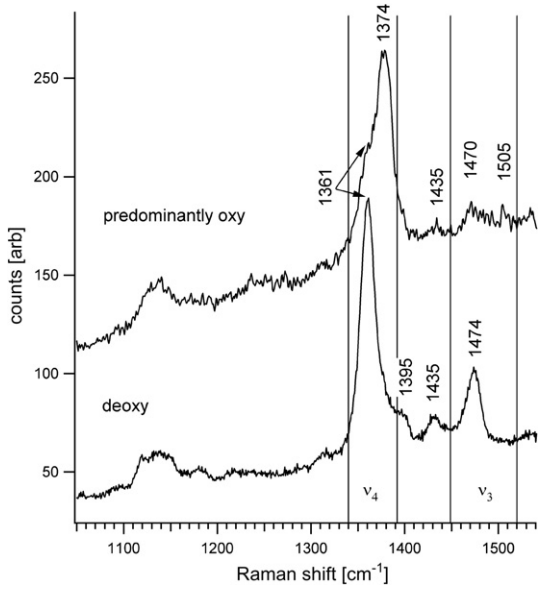

Fig. 2. Resonance Raman spectra of the high wavenumber region from a ganglion of the nerve cord. The power prior of the microscope objective was 0.1 mW and the integration time 30 s. The calculated spectral resolution at 413.1 nm is 10 cm^{-1}. The uppermost spectrum shows an almost oxy spectrum and the spectrum below shows a deoxy spectrum, in order to verify the penta-coordinated high spin and the hexa-coordinated low spin form, respectively. In order to get the deoxygenated state, the nerve cord was exposed to anaerobic buffer. The regions of the ν_3 band and the ν_4 band are marked by straight vertical lines in the graph.

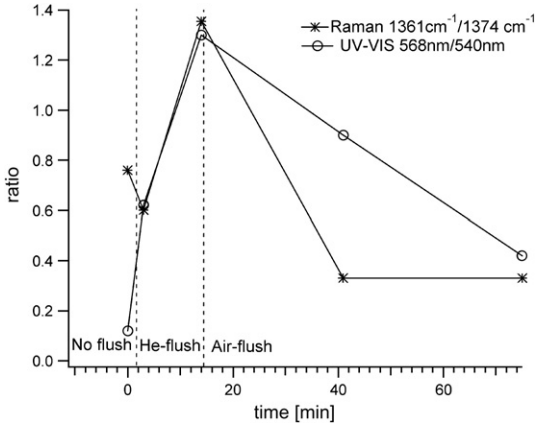

Fig. 3. Combined micro-resonance Raman and absorption spectra of the nerve cord under different aerobic conditions. The resonance Raman-integration time was 20 s, at a power of 0.07 mW prior to the microscope objective. The ratio of the Raman intensities at 1361 cm^{-1} (deoxy) to 1374 cm^{-1} (oxy) is shown. For the absorption spectrum the ratio between absorption values at 568 nm (deoxy) and 540 nm (oxy) are plotted. The dotted vertical lines indicate when the flush was changed from anaerobic to aerobic seawater.

The applied Raman laser power was ~0.07 mW prior to the microscope objective, which is very low and at the cost of a poor signal-to-noise ratio. However, the strong oxidation state marker ν_4 can still be detected and the low laser power gives the advantage that sample degradation effects by photochemistry can be minimized. In order to obtain the right aerobic or anaerobic conditions, the seawater containers (80 ml) were purged for several days with He and dry air before the experiments were started.

The results for both the Raman and the absorption measurements are summarized in Fig. 3. The Raman results are presented by showing the ratio between the intensities of the ν_4 band at 1361 and 1374 cm^{-1} respectively, which indicates the shift from a deoxygenated to an oxygenated or oxidised form. For the absorption measurements the ratio between 568 and 540 nm is shown, which is also a measure of the relative concentration of the deoxygenated form compared to the oxygenated form. Before calculating the ratio, care was taken to rule out the presence of an oxidised form in the sample. The dotted vertical lines indicate when the flushing conditions were changed.

As can be seen in Fig. 3, there is a clear correlation between the resonance Raman and the absorption data. Furthermore, no oxidation of the nerve globin could be observed in the absorption spectrum, as expected when the nerve cord is kept under physiological conditions. When the nerve cord was exposed to different aerobic environments, a shift of peaks was observed in both spectra and the fast reaction to the changing condition points towards an oxygen-carrying/storage function of the protein.

3.3. Pitfalls of the experiment — fluorescence and the observation of a local photo-induced oxygenation cycle

The photo-induced effects of different Raman excitation lines have been studied thoroughly for mammalian Hb. For these heme proteins it was found that the photo-induced

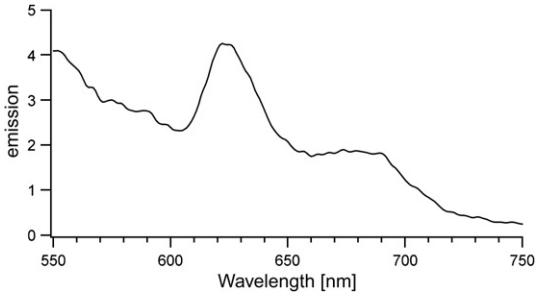

Fig. 4. Fluorescence spectrum of the nerve cord after illumination with 568 nm, indicating the decomposition of the nerve globin to biliverdin. The spectrum is smoothed over 3 points with a binomial algorithm.

degradation of the protein can be delayed considerably when using a laser wavelength of 568 nm or 633 nm instead of 514.5 or 488 nm [24,25]. With these results in mind, we applied the 568 nm laser line for Raman excitation as we started the experiments on the nerve globin. Surprisingly, this resulted in a strong orange–red fluorescent emission visible by the naked eye followed by a significant decrease of the Raman signal. For this reason, the fluorescence spectrum of the nerve cord was measured, which is shown in Fig. 4. The fluorescence spectrum corresponds well to the spectrum of biliverdin, a decay product of the heme [26,27]. The photoproducts are created by the reduction of a double bond and the process involves singlet oxygen, which is the main cytotoxic agent responsible for the photodynamic effect. Hence, the choice of an appropriate Raman excitation wavelength is crucial in order to avoid photo-induced degradation of the specimen.

Furthermore, photo-induced degradation is known to depend on the laser power. Different Raman laser powers were therefore applied and the consequential photochemistry was investigated. The results from measurements at ~0.07 mW, 0.3 mW and 0.9 mW are shown in Fig. 5. For each series, five subsequent spectra were taken and the integration time was set to 20 s. During the measurements, the nerve cord was kept under a constant flow of air-purged seawater. When applying 0.07 mW, the ν_4 line was predominantly apparent at 1374 cm^{-1} (oxy form of the globin) and no change in spectra could be observed over time. Therefore, it is concluded that photochemistry is negligible at this laser power. The spectra taken at 0.9 mW show a full transition to the deoxy ferrous state despite the flushing with oxygen-rich seawater. This shows that this laser power causes a full photo-induced deoxygenation of the protein. When applying an intermediate laser power (0.3 mW), initial de-oxygenation (see appearance of ν_4 band at 1361 cm^{-1}) with subsequent re-oxygenation is observed. Neither the situation at 0.3 mW nor the one at 0.9 mW laser power reflects the native state of the nerve globin under O_2.

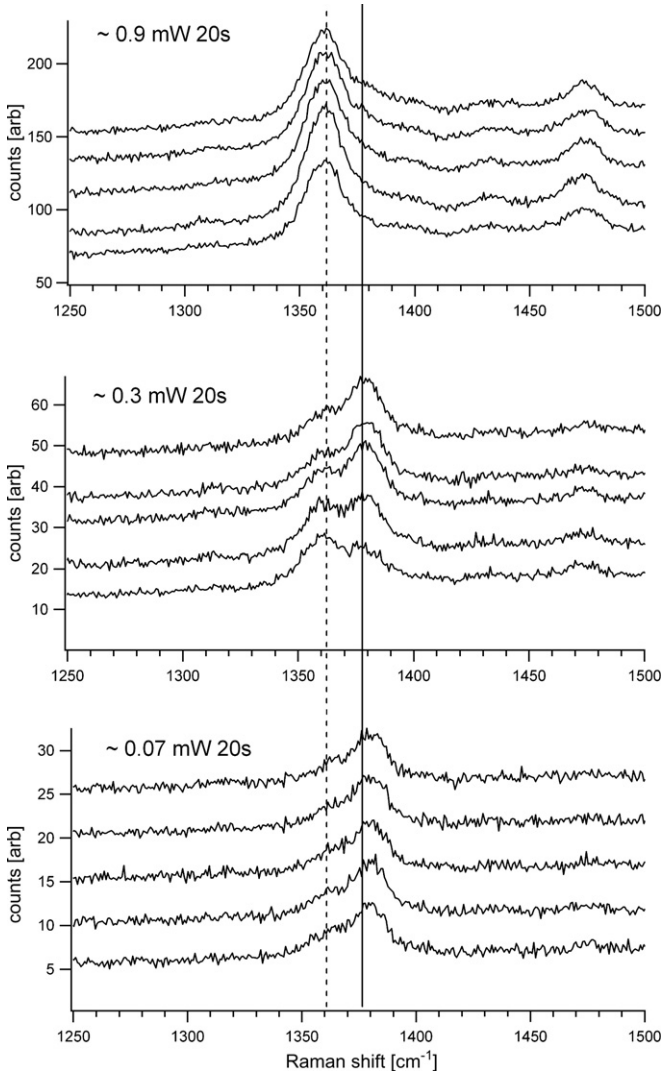

Fig. 5. Testing of different Raman laser powers ~0.07 mW, 0.3 mW and 0.9 mW measured prior to the microscope objective. Integration time was set to 20 s. Bottom trace corresponds to the first measurement of the time series. In all experiments the nerve cords were flushed with oxygen-rich seawater.

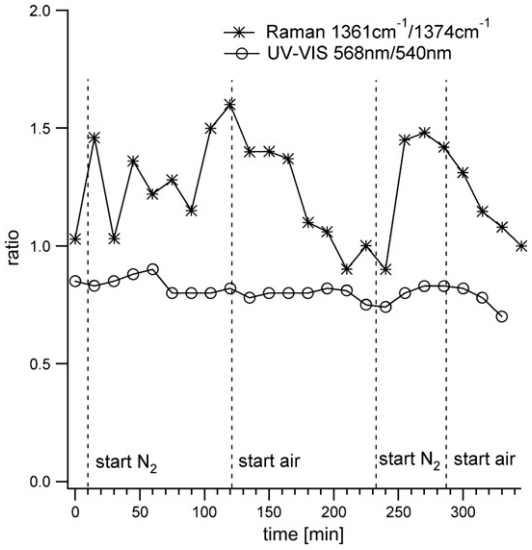

Fig. 6. Combined micro-resonance Raman and absorption data of the nerve cord under different conditions. The experimental data are obtained at higher laser power and with shorter purging times of the seawater than in Fig. 3. Resonance Raman-integration time is 20 s and the power is 0.6 mW. In the graph, the ratio of the Raman intensities at 1361 cm^{-1} (deoxy) to 1374 cm^{-1} (oxy) is shown. For the absorption spectrum the ratio between absorption values at 568 nm (deoxy) and 540 nm (oxy) are plotted.

Finally, we show the importance of combining the resonance Raman detection with absorption spectroscopy to detect possible instrumental-induced spectral changes. Fig. 6 depicts a time series of resonance Raman and UV–Vis experiments, similarly as in the experiment shown in Fig. 3. In this case, however, the seawater containers were purged for only 2 h prior to the experiments and a laser power of 0.6 mW was applied. The shift of the v_4 band from 1374 to 1361 cm^{-1} and back again in the resonance Raman spectra seems to indicate that we are observing a similar effect upon change of the oxygen concentration as reported in Fig. 3. Indeed, when exposed to the N_2-purged seawater, the 1361 cm^{-1} line rises whereas the 1374 cm^{-1} peak decreases and *vice versa*. Surprisingly, the absorption measurements do not corroborate these results. Here, the spectra show that the nerve globin is essentially remaining in the oxy state throughout the whole measurement of 5 h despite of the long flushing with N_2-purged seawater. This clearly indicates that the resonance Raman results are corrupted by laser-induced photochemistry. As in the previous experiments, no oxidation of the sample could be observed despite the long time span, proving again the long *ex vivo* stability of the nerve cord.

4. Discussion

The macro-resonance Raman investigation shows that the nerve globin of the polychaete annelid *A. aculeata* is in a penta-coordinated high spin form when in the ferrous state with the sixth position available for fast binding of exogenous ligands. These results confirm the *in vitro* analyses of the purified protein using absorption spectroscopy [7].

In this work, we show that by combining micro-resonance Raman and absorption spectroscopy with a microfluidic system, it is possible to investigate the oxygenation cycle of the nerve globin *in vivo* in the nerve cord. The time series depicted in Fig. 3 show that the fast reaction of the nerve globin to the varying O_2 concentration indeed points toward an oxygen-carrying/storing function of the nerve globin. This result is consistent with the previous study on the globin and globin gene structure of this nerve heme protein. It was found that based on its intracellular location, its abundance and its functional characteristics, the *A. aculeata* nerve globin most likely functions as an oxygen store or carrier [7,16]. We found that close to the inlet of the flow cell, the transfer between different states was much faster than in the middle of the flow cell, indicating that the flow within the cell is not homogeneous. Indeed, the nerve cord itself probably hindered the flow, as it filled a significant fraction of the cross-section of the cell. This could be improved by having an elongated ellipsoid reservoir instead of a circular one.

The current results open the way to study the action potential of the nerve cord in relation to the oxygenation of the nerve globin under aerobic and anaerobic environments, which is one of the main future applications of the set-up. In the present study we also illustrate some of the pitfalls of the resonance Raman set-up. As becomes apparent from Fig. 5, the laser power plays an important role. It is well known that intense illumination can give rise to local photo-induced chemistry, heating and/or damage to biological macro-molecules [28–34]. On the one hand, several techniques, such as time-resolved spectroscopy have been used to investigate photo-dissociation of heme coordinating CO, O_2 or NO [35]. On the other hand, thermally induced metHb formation has been shown to occur due to the high absorption of the laser illumination by the heme [33].

From Fig. 5 it is clear that a laser power of 0.9 mW induces photo-dissociation of the Fe–O_2 bond, but no thermally induced oxidation of the heme iron. When applying an intermediate laser power (0.3 mW), the spectra are found to change in time (Fig. 5, middle figure). In the first spectrum the deoxy-state is dominating, since the intensity of the 1361 cm^{-1} line is higher than that of the 1374 cm^{-1} line. This indicates that partial photo-induced removal of oxygen has occurred. Interestingly, a return of the protein to its oxygenated state is observed in the subsequent spectra. This indicates that we are observing an intermediate situation where laser-induced de-oxygenation is competing with the oxygenation process. Slight changes in the external condition (small fluctuations in the oxygen concentration, protein diffusion process, small sample movements, etc.) can therefore influence the competition between the two reactions.

The experiment in Fig. 6 illustrated that laser-induced photochemical processes may go unnoticed when compensated by a different error source. Indeed, in this experiment a laser power of 0.6 mW was used (so photo-dissociation was taking place) and the experiment shown in Fig. 3 was repeated using insufficiently N_2-purged seawater (the oxygen concentration was reduced but not zeroed). The resonance Raman analysis seemed to parallel the situation observed in Fig. 3, but was contradicted by the absorption analysis. This can be explained as follows. When laser radiation is tightly focused, as in the present Raman experiment, the photo-induced effects can be very local. Hence the sample is not necessarily entirely affected or damaged. Further, laser light guided through a lens or a microscope objective is focused onto one spot and most of the signal will be collected from a confined area along the depth of the sample with a diameter of ~1.5 μm and a depth of ~5 μm. For the absorption measurements, white light with a wavelength-range between 400 and 680 nm is used. In this case, the illumination is an extended light source and cannot be focused onto a small spot. Therefore, the two methods show different results despite the fact that the same microscope objective has been used and the observations seen in Fig. 6 can be interpreted as follows. Due to the reduced N_2 flushing of the seawater prior to the measurements not all oxygen has been expulsed from the seawater solution leading to the continuous observation of the oxy form of the globin in the absorption spectra. However, when a laser power of 0.6 mW is used, photo-dissociation will compete with the oxygenation reaction. The rate of the oxygenation reaction depends on the concentration of O_2 in the sample. When flushing with air-purged seawater, the oxygenation rate is faster than the photo-dissociation rate. As the concentration of oxygen is lowered in the partially N_2-purged seawater, the rate of the oxygenation becomes smaller and is unable to compete with the photo-dissociation reaction. This explains why a purging-dependent effect is detected using

resonance Raman that does not parallel the absorption results. It also shows that extreme care needs to be taken when interpreting resonance Raman data only.

5. Simplified description of the method and its (future) applications

The combination of micro-resonance Raman and absorption spectroscopy with a microfluidic system is an excellent tool to investigate the response of a specimen to environmental stimuli. The microfluidic system enables a fast and controlled change of the environment surrounding the sample while physiological conditions can be maintained. The subsequent response of the sample towards the changing conditions can be recorded immediately by the spectroscopic techniques applied. Resonance Raman spectroscopy provides more information about conformational changes due to ligand-binding compared to absorption spectroscopy. However, the latter method gives information about the photo-induced degradation of the sample. By combining the two techniques possible misinterpretation of the result can be avoided, while more information can be gained. Moreover, the sample can be studied for extended periods of time. In this report it is demonstrated that resonance Raman and absorption spectroscopy is especially useful when investigating heme proteins. The set-up could also be extended to study changes in the heme ligand-binding of the nerve globin in function of action potentials. Further, the techniques used are not restricted to globins but can be used for almost all biological samples. Hence, the set-up presented here can be valuable for many biomedical applications where the immediate response of a specimen towards variations of the physiological surrounding has to be monitored in real time.

Acknowledgements

This work was supported by the European Commission 6th framework programme through the project ATOM-3D (Contract No. 508952), and from the European Science Foundation EUROCORES Progamme, SPANAS, through funds from the Swedish Research Council and from the European Commission Sixth Framework Programme. Further acknowledged is the Fund for Scientific Research-Flanders (FWO) for support through the Grant G.0468.03 and the European Commission project (Contract No QLG3-CT-2002-01548 to L.M). S. D. and W. W. are postdoctoral fellows of the FWO. For technical assistance we would like to thank Heinrich Riedl and Paul Casteels.

References

[1] Gow AJ, Payson AP, Bonaventura J. J Inorg Biochem 2005;99:903–11.
[2] Pesce A, Bolognesi M, Bocedi A, Ascenzi P, Dewilde S, Moens L, et al. EMBO Rep 2002;3:1146–51.
[3] Weber RE, Vinogradov N. Physiol Rev 2001;81:569–628.
[4] E.R. Lankester, 21 (1872) 70–81.
[5] Wittenberg BA, Briehl RW, Wittenberg JB. Biochem J 1965;96:363–71.
[6] Wittenberg JB. Adv Comp Environ Physiol 1992;13:60–85.
[7] Dewilde S, Blaxter M, Van Hauwaert M-L, Vanfleteren J, Esmans EL, Marden M, et al. J Biol Chem 1996;271:19865–70.
[8] Hundahl C, Fago A, Dewilde S, Moens L, Hankeln T, Burmester T, et al. FEBS J 2006;273:1323–9.
[9] Kraus DW, Colacino JM. Science 1986;232:90–2.
[10] Walker GM, Zeringue HC, Beebe DJ. Lab Chip 2004;4:91–7.
[11] Beebe DJ, Mensing GA, Walker GM. Annu Rev Biomed Eng 2002;4:261–86.
[12] Fujii T. Microelectron Eng 2002;61–62:907–14.
[13] Spiro TG, Strekas TC. J Am Chem Soc 1974;96:338–45.
[14] Strekas TC, Spiro TG. Biochim Biophys Acta 1972;263:830–3.
[15] Brunner H, Sussner H. Biochim Biophys Acta 1973;310:20–31.
[16] Geuens E, Dewilde S, Hoogewijs D, Pesce A, Nienhaus K, Nienhaus GU, et al. IUBMB Life 2004;56:653–6.
[17] Egawa T, Yeh S-R. J Inorg Biochem 2005;99:72–96.
[18] Podstawka E, Proniewicz LM. J Inorg Biochem 2004;98:1502–12.
[19] Sun J, Wilks A, Ortiz de Montellano PR, Loehr TM. Biochemistry 1993;32:14151–7.
[20] Van Doorslaer S, Trandafir VEF, Ioanitescu I, Dewilde S, Moens L. IUBMB Life 2004;56:665–70.
[21] Couture M, Burmester T, Hankeln T, Rousseau DL. J Biol Chem 2001;276:36377–82.
[22] Uno T, Ryu D, Tsutsumi H, Tomisugi Y, Ishikawa Y, Wilkinson AJ, et al. J Biol Chem 2004;279:5886–93.
[23] Dewilde S, Kiger L, Burmester T, Hankeln T, Baudin-Creuza V, Aerts T, et al. J Biol Chem 2001;276:38949–55.
[24] Wood BR, McNaughton D. J Raman Spectrosc 2002;33:517–23.
[25] Ramser K, Logg K, Goksör M, Enger J, Käll M, Hanstorp D. J Biomed Opt 2004;9.
[26] König K, Schneckenburger H, Rück A, Steiner R. J Photochem Photobiol B Biol 1993;18:287–90.
[27] Rotomskis R, Streckyte G, Bagdonas S. J Photochem Photobiol B Biol 1997;39:172–5.
[28] Puppels GJ, Olminkhof JHF, Segers-Nolten GMJ, Otto C, DeMul FFM, Greve J. Exp Cell Res 1991;195:361–7.
[29] Ramser K, Bjerneld EJ, Fant C, Käll M. J Biomed Opt 2003;8:173–8.
[30] Liang H, Vu K, Krishnan P, Trang T, Shin D, Kimel S, et al. Biophys J 1996;70:1529–33.
[31] Neuman KC, Chadd EH, Liou GF, Bergman K, Block S. Biophys J 1999;77:2856–63.
[32] Ramser K, Enger J, Goksör M, Hanstorp D, Logg K, Käll M. Lab Chip 2004;5:431–6.
[33] Randeberg LL, Bonesronning JH, Dalaker M, Nelson JS, Svaasand LO. Lasers Surg Med 2004;34:414–9.
[34] Nöllmann M, E.P. Spectrochim Acta Part A 2000;56:2817–29.
[35] Nienhaus GU, Mourant JR, Chu K, Frauenfelder H. Biochemistry 1994;33:13413–30.